

Strong-Field Photoionization by Few-Cycle Laser Pulses

Gerhard G. Paulus

Abstract. The electric field of few-cycle laser pulses can be precisely controlled by controlling their “absolute” phase. Intense phase-stabilized few-cycle laser pulses give rise to novel effects in strong-field and above-threshold ionization (ATI). The phase dependence of the photoelectron spectra is a sensitive probe of the dynamics of the strong-field ionization processes underlying attosecond laser physics. Conversely, the phase-dependence of ATI spectra can be used for the measurement of the absolute phase. This, a summary of the experimental status of phase-dependent strong-field ionization, and a description of unsolved problems are the main points of this contribution.

2.1 Introduction

Attosecond XUV- and electron pulses can be generated by interaction of intense ultra-short laser pulses with atoms and also with molecules. This is remarkable as the optical period of the commonly used lasers is 2.5 fs long which means that the processes leading to the attosecond pulses not only must evolve within an optical cycle, but also be precisely synchronized to the driving optical field. The key for understanding attosecond laser physics is understanding strong-field photoionization. It has been shown in the last decade of the twentieth century that all of the characteristic effects observed in strong-field laser–atom interaction – namely the plateaus in high-harmonic generation (HHG) [1] and above-threshold ionization (ATI) [2] as well as the knee in non-sequential double-ionization [3] – are due to a class of trajectories of photo-ionizing electrons that are driven back to the vicinity of the core by the oscillating laser field [4–6], for reviews see [7–9]. Depending on the instant of ionization and return, these electrons may hit the ion core with attosecond timing precision and with energies up to $3.17 U_P$, where U_P is the ponderomotive energy [4]. Even at the nowadays fairly modest intensity of $10^{14} \text{ W cm}^{-2}$, the ponderomotive energy is 6 eV (again assuming 800 nm wavelength). Therefore, high-harmonics, in fact XUV attosecond pulses, can be generated in the

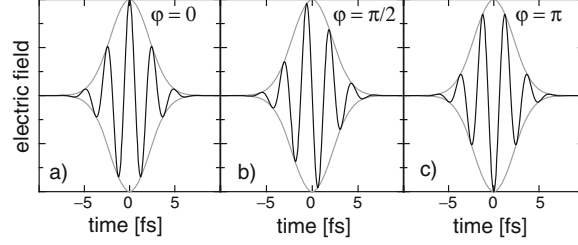


Fig. 2.1. 5-fs laser pulses consist of less than two optical cycles (few-cycle pulses). The temporal evolution of the electric field of such pulses depends on the phase of the carrier with respect to the envelope, the so-called carrier-envelope (CE) phase or “absolute” phase. By convention, the origin of the time scale is chosen to be at the maximum of the envelope of the pulses. Then an absolute phase $\varphi = 0$ corresponds to cosine-like pulses and $\varphi = -\pi/2$ to sine-like pulses. [20]

case the returning electron makes a transition to the ground state. Impact ionization leads to non-sequential double-ionization [5], and elastic scattering to the ATI plateau [6,10]. Although numerous experiments have revealed some serious deficits of this essentially classical picture of strong-field laser–atom interaction, the model has proven to be a very useful guiding principle. This also holds with respect to synchronization of the attosecond pulses with the driving field.

The very fact that the dynamics of strong-field ionization and attosecond pulse generation proceed within and are phase-locked to single optical cycles suggests that it is highly desirable to use as few optical cycles for the driving field as possible [11,12]. One immediate benefit are isolated attosecond pulses whereas longer pulses lead to trains of, in general, not identical attosecond pulses. If the duration (FWHM) of the driving pulses can be reduced to less than three optical cycles (few-cycle pulses), it is in addition possible to tailor the optical cycles by controlling the phase (“absolute” phase) of the carrier oscillation with respect to the maximum of the pulse envelope. This facilitates direct control of the electron trajectories responsible for attosecond pulse generation and works the better the shorter the driving pulse. The absolute phase φ obviously plays a key role in attosecond laser physics. For an unambiguous definition, the field $\mathcal{E}(t)$ of the laser pulse is written as a product of envelope $\mathcal{E}_0(t)$ and carrier wave:

$$\mathcal{E}(t) = \mathcal{E}_0(t) \cdot \cos(\omega t + \varphi). \quad (2.1)$$

This definition also explains the frequently used jargon of sine- and cosine-like pulses which are just special cases of few-cycle laser pulses.

The pivotal importance of the absolute phase for attosecond laser physics and other modern branches of laser physics explains the many proposals and attempts to devise a scheme for its measurement [13–18]. In this paper we discuss strong-field photoionization, i.e., above-threshold ionization, by few-cycle pulses. Some of the results are directly relevant for attosecond science

as they address the dynamics of strong-field photoionization, others for the application of ATI for phase measurement. This paper concentrates on experimental aspects, unsolved problems, and phase measurement. A review on the entire scope of ATI with few-cycle laser pulses can be found in [19]. ATI offers numerous possibilities for phase-measurement and investigation of few-cycle strong-field ionization if the number of electrons emitted in positive (“right”) and negative (“left”) direction is compared.¹ For phase measurement it is important to realize that the requirements are manifold:

- The effect needs to exhibit a strong asymmetry, ideally in an energy range where the count rate is high.
- The dependence of the effect on the absolute phase should be known with high accuracy.
- The phase dependence (e.g., the phase at which there is equal count rate on the left and the right detector) should not depend on intensity, pulse duration, etc. Otherwise re-calibration is necessary as conditions change or errors occur if changes go unnoticed.
- Ideally the degree of asymmetry can be used for a measurement of the pulse duration. This, however, requires a particularly good understanding of the underlying physical mechanisms.

2.2 Detection of the “Absolute” Phase

The most conspicuous feature of few-cycle pulses is their asymmetry. Assuming the conditions implied by (2.1) a cosine-like pulse exhibits mirror-symmetry at $t = 0$ while sine-like pulses exhibit inversion symmetry. It is important to realize that the symmetry or lack of thereof refers to a single optical cycle: Shaping pulses is not new unless the envelope is shaped such that it changes considerably within one optical cycle. In this sense all long pulses exhibit mirror and inversion symmetry. As a consequence of the Curie principle, the photoelectron angular distribution exhibits at least inversion symmetry as long as we accept the approximation that strong-field ionization is essentially a single-cycle process. This symmetry can be broken by few-cycle laser pulses, provided ionization is a highly non-linear process. (Linear photoionization cannot lead to asymmetric photoionization because the integral of the field of a propagating electromagnetic pulse must be zero.)

The broken inversion symmetry of photoelectron angular distributions is equivalent to a negative correlation (or anti-correlation) of photoelectrons emitted in opposite directions. The significance of this insight is that phase-stabilized amplified few-cycle pulses are not necessary for the detection of phase effects. Rather, correlations can be detected – actually with very high

¹ Throughout this paper it is assumed that only electrons emitted parallel to the polarization are detected unless otherwise noted.

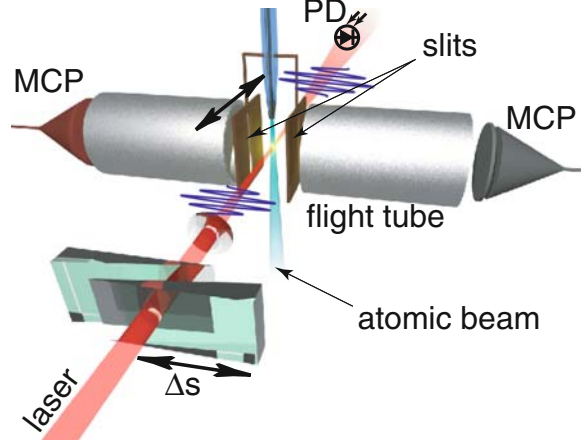


Fig. 2.2. *Stereo-TOF spectrometer.* Two opposing flight tubes are mounted inside a ultra-high vacuum apparatus. Atoms or molecules can be fed in through a glass nozzle and are ionized by a focussed few-cycle laser pulse (in reality, reflective optics is used). A pair of slits, which can be moved with a vacuum manipulator, transmits only electrons ionized in a small fraction of the focus. The absolute phase can be changed either by moving the pair of slits (Gouy effect) or by moving one of the glass wedges thus changing glass dispersion. [42]

sensitivity – by analyzing shot for shot the electron yield recorded by two electron detectors positioned at the left and the right of the laser focus. Due to its characteristic scheme, the instrument is referred to as a stereo-ATI spectrometer, see Fig. 2.2. Each laser pulse results in a pair of integers representing the number of electrons detected for this pulse on the left and the right electron detector. After accumulating data for 10^5 – 10^6 laser pulses a two-dimensional histogram, which represents the probability distribution of the pairs of integers, i.e., the electrons detected simultaneously on the left and the right detector, can be produced, typically presented in false-color coding. In such a contingency (or correlation) map, anti-correlations show up as structures perpendicular to the diagonal: If a certain pulse produces many electrons emitted to the left, then there is a high probability that only a few electrons will be emitted to the right, and vice versa. This exactly has been measured for Krypton atoms exposed to 780-nm circularly polarized laser pulses of 6–7 fs pulse duration (FWHM) and $5 \times 10^{13} \text{ W cm}^{-2}$ intensity [20], see Fig. 2.3. A weaker anti-correlation has been found for linear polarization.

The correlation method was also investigated theoretically [21]. For this calculation a Keldysh-type model [22] was adapted to few-cycle pulses. One result has been the dependence of the strength of anti-correlation as a function of pulse duration. An earlier prediction [23] that circular polarization leads to stronger inversion asymmetries was confirmed qualitatively. The theoretical modeling also addressed the central problem of the correlation approach:

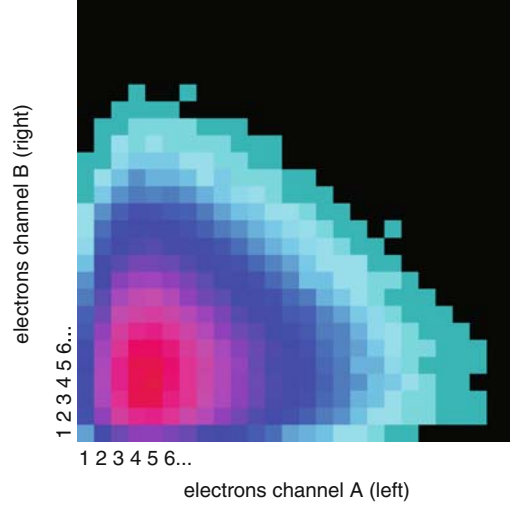


Fig. 2.3. Evidence of absolute-phase effects from few-cycle laser pulses. In this contingency map, every laser shot is recorded according to the number of photoelectrons measured in the left and the right arm of the stereo-ATI spectrometer. The number of laser shots with electron numbers according to the coordinates of the pixel is coded in grey shades. The signature of the absolute phase is an anticorrelation in the number of electrons recorded with the left and the right detector. In the contingency map they form a structure perpendicular to the diagonal [20]. Shown here is a measurement with krypton atoms for circular laser polarization, a pulse duration of 6 fs, and an intensity of $5 \times 10^{13} \text{ W cm}^{-2}$. [20]

Laser pulse fluctuations create positive correlations. Due to the non-linear dependence of multi-photon ionization probability on intensity, even modest laser pulse fluctuations create positive correlations that can mask the effects of the absolute phase. Also this finding agrees well with the experimental evidence.

2.3 Asymmetric Ionization

We now proceed with a quantitative analysis of the energy-integrated photoelectron yield in opposite directions and parallel to the laser polarization. It may be instructive to start the discussion with a naive and in fact essentially wrong model: The asymmetry $R(\varphi)$ defined as the ratio of the energy-integrated (“total”) electron yield to the left and to the right is estimated using the quasi-static tunneling ionization probability [24, 25]

$$P_{\text{ion}}(t) \propto \left(\frac{2\kappa^3}{|\mathcal{E}(t)|} \right)^{2/\kappa-1} \exp \left[-\frac{2\kappa^3}{3|\mathcal{E}(t)|} \right], \quad (2.2)$$

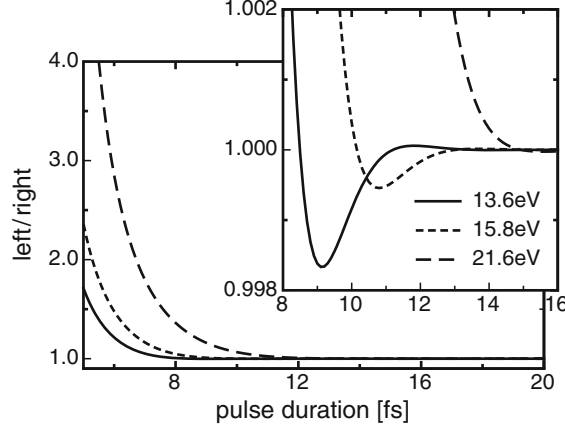


Fig. 2.4. Asymmetry of photoelectron yield calculated by integrating static tunneling ionization probabilities for positive and negative sign of the field. The result of this oversimplified model is shown as a function of pulse duration and ionization potential. The inset shows that the function is not quite monotonic. The intensity used was $10^{14} \text{ W cm}^{-2}$

where $\kappa^2 = 2E_{\text{Ion}}$ with E_{Ion} being the ionization threshold. With the suggestive (but invalid!) assumption that electrons generated at instants where the field had opposite sign would travel to opposite directions, the yield on the left and on the right detector would be estimated by integrating $P_{\text{ion}}(t)$ for positive and negative sign of the field separately. The ratio $R_{\text{max}} = \max(R(\varphi))$ of the yield for left and right direction (“asymmetry”) calculated in this way is shown in Fig. 2.4 in dependence of the pulse duration. The asymmetry is a steep function of pulse duration and ionization threshold, as expected. This suggests that $R(\varphi)$ can be used not only for phase measurement, but also for determining the pulse duration with the remarkable feature of increasing sensitivity with decreasing pulse duration. It will turn out that this promise is not kept.

The oversimplification of the above model comes from the fact that an electron that tunnels at an instant $t = t_0$ will be deflected by the subsequent evolution of the field. Invoking the strong-field approximation which assumes that the field does not affect the ground state and the atomic potential does not affect electrons in the continuum, it is straightforward to predict the emission direction of the electron. From conservation of canonical momentum $\mathbf{p}_{\text{can}} = \mathbf{p} - e\mathbf{A}(t)$, one finds that the electron will be emitted in the opposite direction of the vector potential \mathbf{A} at the instant of tunneling t_0 . An assumption used is that the electron momentum at $t = t_0$ is negligible. The fact that the vector potential of a sine-like pulse is essentially cosine-like and vice versa, together with the fact that the tunneling probability is of course still be given by the field strength $\mathcal{E}(t_0)$, has two consequences: (a) the most asymmetric pulse shape, i.e., cosine-like pulses, will lead to symmetric yield, i.e., the same number of electrons on the left and the right detector:

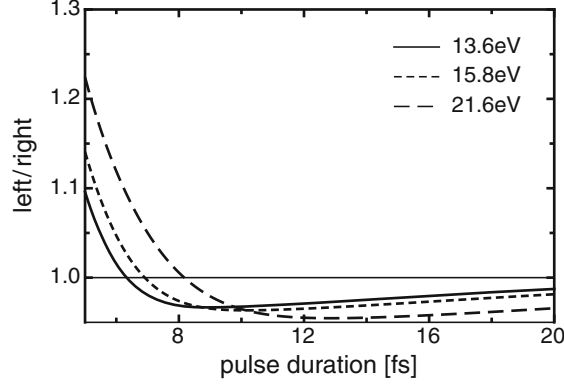


Fig. 2.5. Asymmetry of photoelectron yield calculated by the classical model of strong-field ionization for the same conditions as in Fig. 2.4

$R_{\max} = R(\pm\pi/2)$, $z = R(n\pi)$, $n \in \mathbb{Z}$ (b) The strength of the asymmetry will be greatly reduced, see Fig. 2.5. An illustration of the latter effect can be found in [26].

It is interesting to note that the asymmetry as a function of pulse duration changes sign for both models considered with the effect being more pronounced for the “correct” model, see Figs. 2.4 and 2.5. The experimental evidence (see Fig. 2.7) reveals however that the classical model is wrong in predicting equal electron yield to the left and to the right for cosine-like pulses. This result was confirmed by theoretical investigations based on numerical solutions of the time-dependent Schrödinger equation (TDSE) [27]. For typical conditions (6 fs, $0.7 \times 10^{14} \text{ W cm}^{-2}$) symmetric electron yield is generated at a phase $\varphi \approx -0.3\pi$. However, other phase dependencies of R are also observed. The attempt to establish a relationship between left–right contrast and pulse duration by solving the TDSE for various pulse lengths leads to a surprisingly complex picture, see Fig. 2.6. If we try to model the logarithm of $R(\varphi)$ by a sine-like function, we would make the ansatz

$$\log R(\varphi) = \log R_{\max} \cdot \sin(\varphi + \bar{\varphi}). \quad (2.3)$$

If the classical model were correct, $\bar{\varphi} = 0$. However, Fig. 2.6 indicates that $\bar{\varphi}$ can assume any value and R_{\max} depends on intensity and, as more detailed calculations reveal, pulse duration in a non-trivial way. It appears that the asymmetry $R(\varphi)$ of the energy-integrated photoelectron yield is not a reliable indicator for the absolute phase. In addition, $R(\varphi)$ cannot be used for estimating or measuring the pulse duration. This conclusion is drawn from calculations using a 1D model atom. 3D calculations can certainly be expected to deliver a quantitatively different result. Qualitatively, however, the above conclusion can be expected to be valid in consideration that results of 3D calculations do also result in a complicated dependence of R on intensity, pulse duration, etc. [28–30]. Although it is obvious that the strong-field

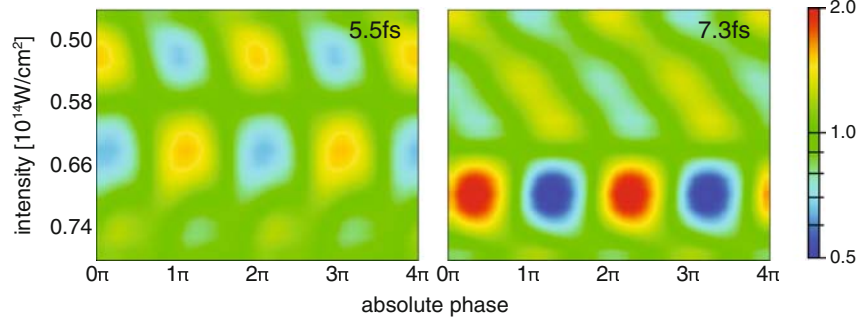


Fig. 2.6. The left-right ratio of the energy-integrated photoelectron yield as a function of the phase φ and intensity. The figure displays the result for a 1D model atom for 5.5 and 7.3-fs pulses. As the pulse duration is increased, the pattern changes gradually and moves in direction of lower intensities. For comparison to experiment, focal averaging needs to be taken into account, i.e., averaging over a range of intensities

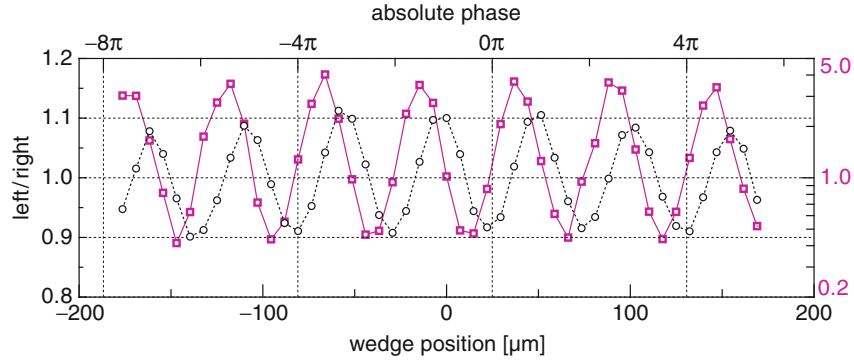


Fig. 2.7. Measurement of $R(\varphi)$ (*open dots*). The phase φ was changed by shifting one of the glass wedges (see Fig. 2.2). The *open-square* data points correspond to ATI plateau electrons that will be discussed in Sect. 2.4.2

approximation, i.e., neglecting the atomic potential, is responsible for the discrepancies of analytical and numerical results, the underlying mechanisms of the intricate dependencies of the simplest of all quantities that can be used to characterize asymmetric ionization are not at all clear. It seems, however, that the non-monotonic behavior that can be observed in the simple classical model contributes to the effects.

2.4 Above-Threshold Ionization Spectra

So far only the energy-integrated (or total) yield has been considered. We now turn our attention to energy-resolved spectra. A characteristic of strong-field ionization is that more photons than necessary for ionization may be

absorbed by an atom which leads to correspondingly high electron kinetic energies (above-threshold ionization, ATI) [31].

Phase-dependent photoelectron spectra can only be measured if the absolute phase can be kept constant for many laser pulses, unless the spectrometer is constructed such that a complete spectrum can be measured for a single laser pulse. Single-shot operation is possible, however, it compromises dynamic range and energy resolution. An important development has been the invention of a technique (self-referencing or f -to- $2f$ technique) allowing the use of femtosecond lasers as frequency rulers in precision metrology [13, 14]. This innovation had profound consequences also for time-domain applications like strong-field ionization, high-harmonic generation, and in particular attosecond science. The reason is that stabilizing a femtosecond laser's frequency comb implies that the rate with which the absolute phase changes is stabilized, too. For a review see [32]. In 2003 the self-referencing technique was implemented in a femtosecond laser amplifier [33, 34] thus opening the full potential of tailored few-cycle pulses for time-domain applications. It should be noted that phase stabilization by the f -to- $2f$ technique may lead to small drifts of the absolute phase due to dispersion [35].

Figure 2.8 displays a series of ATI spectra measured for different absolute phases. Although the absolute phases (and thus also the temporal evolution of the electric fields) of the respective pulses are displayed in this set of figures, it should be noted that they are not known a priori. What is known, however, is the difference in absolute phase for each measurement relative to, e.g., the first one. This is because the phase is changed by changing the amount of glass in the laser beam, c.f. Fig. 2.2. From the dispersion properties of the inserted glass found in the literature, it is straightforward to calculate the phase change: A piece of glass of thickness d induces a change $\Delta\varphi$ of the absolute phase given by

$$\Delta\varphi = \omega d \left(\frac{1}{v_{\text{ph}}} - \frac{1}{v_{\text{g}}} \right), \quad (2.4)$$

where v_{ph} and v_{g} are phase and group velocity, respectively.

$$v_{\text{ph}} = \frac{c}{n}, \quad (2.5)$$

$$v_{\text{g}} = \frac{c}{n} + \frac{c\lambda}{n^2} \frac{\partial n}{\partial \lambda}, \quad (2.6)$$

where c is the vacuum speed-of-light and n the refractive index. This means that, at the central wavelength $\lambda_0 = 760 \text{ nm}$ of the laser used in our experiments, a fused silica glass plate with a thickness $d = 26 \mu\text{m}$ changes the absolute phase by $\Delta\varphi = \pi$. A cosine-like pulse would be converted into a minus-cosine-like pulse.

The ATI spectra displayed in Fig. 2.8 exhibit a typical structure that is well-known from longer pulses: The electron yield decreases steeply with increasing energy. For intensities exceeding $0.5 \times 10^{14} \text{ W cm}^{-2}$ this drop comes

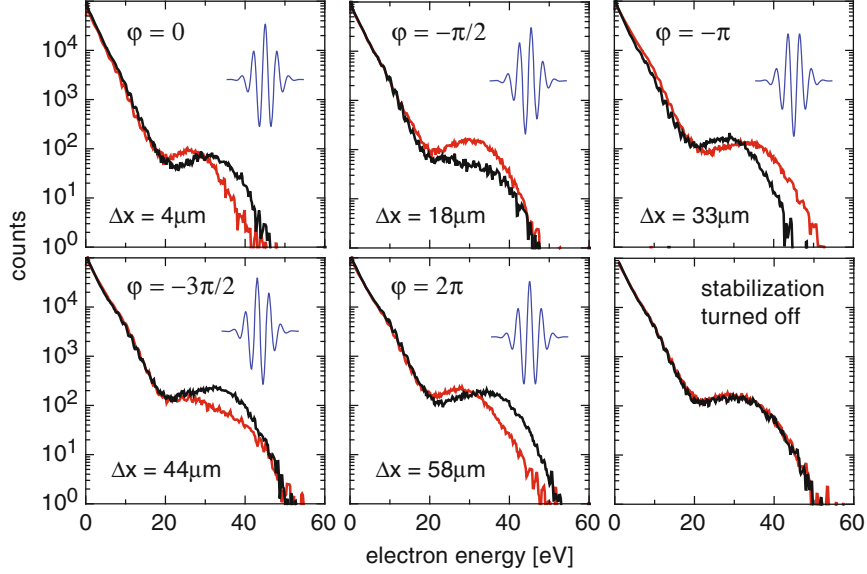


Fig. 2.8. Xenon photoelectron spectra for different absolute phases controlled by fine movement of one of the wedges. Δx indicates the glass added hereby. The *black curves* correspond to emission to the right (positive direction), the *gray ones* to the opposite direction. The inset shows the corresponding real time variation of the electric field, as deduced from comparison of the phase-dependence of the plateau electrons with theory. Only without phase stabilization were identical spectra measured left and right

to a sudden hold at 20–30 eV and a plateau-like structure develops [2]. This means an approximately constant electron yield up to the cut-off energy where the yield decreases in an essentially exponential way again. The phenomenon has already been mentioned in the introduction. It is due to electrons that re-collide elastically with the ion core. In the case of backscattering, the electron velocity is altered such that the electron will be further accelerated in the oscillating electric field of the laser after the re-collision event. For long pulses classical and quantum calculations predict a cutoff energy of $10 U_P$ in good agreement with experimental evidence [6, 36]. An ATI spectrum therefore consists of high-energy (plateau) electrons that underwent rescattering and low-energy electrons that left the atom directly, i.e., without rescattering. Consequently the latter are often referred to as “direct” electrons.

There are a few obvious consistency tests for these measurements: Changing the absolute phase π should result in identical spectra. This is fulfilled to a large extent, but not completely. The reason is that adding glass into the beam not only changes the absolute phase, but also higher-order dispersion that affects the pulse duration. Similarly, changing the phase by π reverses the roles of left and right. From the experimental data it is obvious that the strongest phase effects occur for high-energy (>20 eV) photoelectrons.

However, there are also noticeable phase effects for the low-energy electrons which are difficult to see in Fig. 2.8 due to the semi-logarithmic scale used. A comparison of the asymmetry for direct and rescattered electrons can be seen in Fig. 2.7. In fact, Figs. 2.8 and 2.7 display data from the same experimental run. The curves of Fig. 2.7 correspond to energy-integrated yields where the integration extended from 0 to 50 eV for the open dots and from 20 to 50 eV for the open squares.

A non-trivial observation is that there is no phase for which the spectra measured on the left and the right would be identical – at least for high-energy electrons. This immediately suggests that the processes underlying the ATI plateau electrons are not instantaneous but extend over an appreciable fraction of the laser pulse. Obviously, this conclusion is in perfect agreement with the present understanding of re-collision effects like the ATI plateau.

2.4.1 Low-Energy (Direct) ATI Electrons

The direct electrons are particularly simple to model, at least in the framework of the classical model [37]. From conservation of canonical momentum (cf. Sect. 2.3) and the assumption that the electron has zero momentum at the exit of the tunnel, i.e., $\mathbf{p}_0 := \mathbf{p}(t_0) = 0$, we immediately arrive at the conclusion that the maximum electron energy for a few-cycle laser pulse is $2U_P$ and is obtained for sine-like pulses which have cosine-like vector potentials.² It is of course the hallmark of few-cycle laser pulses that the cutoff energy becomes phase-dependent. Its variation with phase and pulse duration is shown in Figs. 2.9 and 2.10.

Although the existence of the $2U_P$ cutoff has been impressively demonstrated by Gallagher in microwave ionization experiments of Rydberg atoms [38]³, it seems to be hardly known that the effect can also play a role at 800 nm. In fact, there are hardly any measured spectra in the literature that prove its significance for, e.g., rare gas atoms. The reasons may be the following: The ionization yield between 0 and $2U_P$ drops quickly. This can even be understood with the classical model because the higher the electron energy, the smaller the electric field at $t = t_0$, the instant at which the electron enters the continuum. The sharp classical cutoff at $2U_P$ is replaced by an exponential roll-off due to quantum (essentially tunneling) effects. The slope of the spectrum in

² The ponderomotive energy is the cycle-averaged kinetic energy of an otherwise free electron in an oscillating electric field and is given by $U_P = I/(4\omega^2)$ in atomic units. I is the laser intensity and ω the laser angular frequency. The definition of U_P is ambiguous for laser pulses, in particular for few-cycle pulses. Using the maximum of the pulse envelope for I results in a definition that connects seamlessly to long pulses and therefore is used here.

³ The microwave experiments were long-pulse experiments. Due to ponderomotive acceleration the $2U_P$ cutoff then is shifted to $3U_P$.

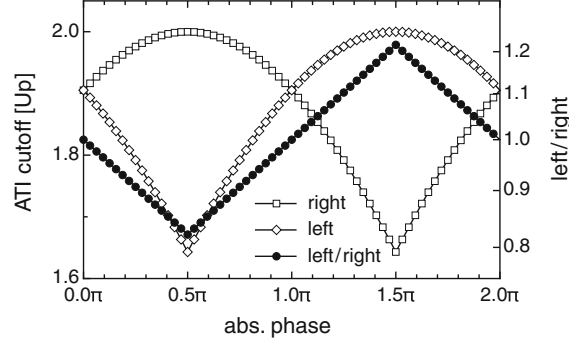


Fig. 2.9. Phase-dependence of the cutoff energy of direct electrons for 2-cycle pulses, i.e., 5.3 fs pulse width (FWHM) at 800 nm. The curves with the open points show the cutoff energy in units of U_P for the spectra measured with the left (*diamonds*) and the right (*squares*) detector. The curve with the solid points displays the ratio of the afore-mentioned curves. Note the logarithmic scale for this curve

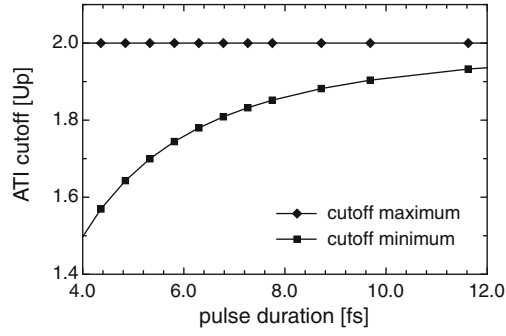


Fig. 2.10. The maximum and minimum cutoff energy as a function of pulse duration. The maximum for electrons emitted to the right is obtained at $\varphi = 0.5\pi$ and the minimum at $\varphi = 1.5\pi$ as shown in Fig. 2.9 for the example of 2-cycle pulses. The $2-U_P$ maximum for the cutoff as well as the phase for which this maximum is obtained are immediate consequences of the strong-field approximation

the classically forbidden region is the steeper the higher the intensity, i.e., the more the classical the situation.⁴

If the slopes of the spectrum for energies smaller and larger than $2U_P$ happen to be similar, the $2-U_P$ cutoff cannot be recognized. This is generally the case for intensities smaller than $10^{14} \text{ W cm}^{-2}$ because the classically allowed energy region ($E < 2U_P$) is small and the slope in the classically forbidden region ($E > 2U_P$) is not very steep. Exposing atoms to significantly higher intensities, on the other hand, often leads to spectra that are difficult to

⁴ It is helpful to use an energy scale in units of the ponderomotive potential for the spectra in order to clearly see the effect.

interpret due to saturation of ionization and focal averaging. Few-cycle laser pulses help avoiding these problems to a certain degree and, in fact, the effect can be seen for ATI spectra generated by sub-10-fs pulses [39]⁵ and obviously also in computer experiments, see e.g., Fig. 5 in [36].

For phase-stabilized few-cycle pulses, the phase-dependence of the $2-U_P$ cutoff has also been observed [35, 40]. Considering the potential of the effect for measuring the absolute phase, it should be noted that the left–right asymmetry can be very significant, much greater than the one for the total yield. Plateau electrons, which will be discussed in the following section, have a comparable if not higher asymmetry. However, their yield is lower by about a factor of 100. Another very important advantage is that the phase dependence of direct electrons beyond the $2-U_P$ cutoff follows closely the classical model as shown in Figs. 2.11 and 2.12. It may sound ironic if not contradictory that the classical model fails badly in reproducing the phase dependence in the classically allowed energy region but does have some predictive power for electrons of classically forbidden energy. Their relatively high energy suggests however that their physics is much less involved than for low-energy electrons. This is confirmed by computer simulations. It should be mentioned that the asymmetry is not only a function of pulse duration but certainly at least also of the energy interval selected and, considering the discussion in the previous paragraph, the laser intensity (higher intensities lead to stepper cutoffs). Therefore, spectral resolution for a phasemeter based on this effect is necessary.

It is apparent from Figs. 2.11 and 2.12 that the classically forbidden electrons can also serve as an excellent probe for measuring the duration of pulses of less than 7 fs duration (FWHM) if the spectra are sufficiently well characterized. While the contrast for longer pulses is still sufficient, the method breaks down due to effects reminiscent of those discussed in Sect. 2.3. Although 3D simulations yield results in general agreement with the ones presented here [28–30], quantitative discrepancies are possible. The experimental results suggest in fact a less complicated behavior than the simulations. This may be due to focal averaging or deficiencies even in the 3D calculations: the only atom for which exact simulations are possible is Hydrogen. However, for Hydrogen no experimental data exists.

2.4.2 High-Energy (Plateau) ATI Electrons

The phase-dependent spectra of high-energy or plateau electrons are fundamentally different from low-energy electrons. An indication of that is the already mentioned fact that there is no phase for which spectra measured

⁵ It is worthwhile to mention that the $2-U_P$ cutoff was observed for Argon. Apparently, the reason is that the slope of Argon spectra is steeper for energies above $2U_P$ than for other rare gases. This fact is known since the discovery of the ATI plateau [2] but has remained unexplained to the present day.

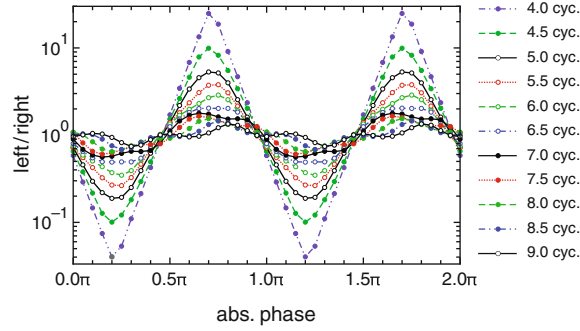


Fig. 2.11. Asymmetry of ATI electrons beyond the $2-U_P$ cutoff (30–40 eV) for various pulse durations. The data was obtained by solving the TDSE for a 1D model atom with an ionization threshold corresponding to Argon. The intensity is $1.8 \times 10^{14} \text{ W cm}^{-2}$ ($2U_P \approx 21 \text{ eV}$)

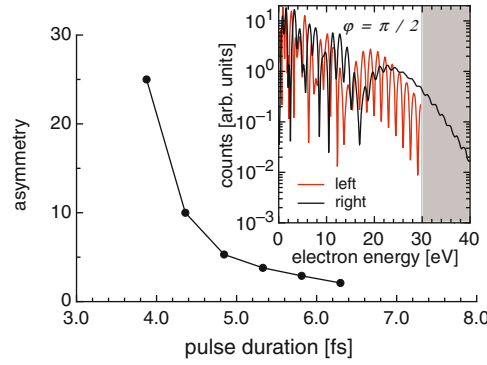


Fig. 2.12. The amplitude of the curves of Fig. 2.11, i.e., the maximum asymmetry, as a function of pulse duration. The inset displays an example of the pairs of spectra from which the other data displayed in Fig. 2.11 and this figure were derived

in opposite directions would be identical. This as well as the high contrast of phase effects for ATI-plateau electrons can be understood in the following way: First of all, high-energy electrons returning to the ion core can only be created in sub-femtosecond time intervals close to peaks of the electric field of the laser pulse. However, the probability that they tunnel through the atomic potential at t_0 depends exponentially on the field strength $\mathcal{E}(t_0)$ and – as few-cycle pulses are involved – it is likely only for those very few optical half-cycles close to the pulse maximum. Generally, the highest kinetic energies are reached for electrons returning to the core at $t = t_1$ such that the electric field becomes nearly zero ($\mathcal{E}(t_1) = 0$). For few-cycle pulses, in addition, the field amplitude \mathcal{E}_0 needs to be as high as possible for $t > t_1$ in order to allow efficient acceleration after rescattering. Since the start time t_0 and return

time t_1 differ by about 75% of one optical cycle, both conditions – namely the highest possible field strength at t_0 and highest possible amplitude after t_1 – are hard to meet and result in a strong dependence of photoionization on the absolute phase. Number, strength, and timing of the wave-packets lead to distinctive structures in the ATI spectra. Their analysis therefore provides detailed information about the key processes of attosecond science. Generally, quantum mechanical calculations are in good qualitative agreement with this classical treatment [41].⁶

The ATI plateau is interesting with respect to phase measurement because the phase-dependence in this part of the spectrum is particularly strong. In addition, in some sense similarly to classically forbidden direct electrons, the influence of the atomic potential on the ATI plateau electrons is small. Therefore even a classical simulation can lead to a meaningful calibration for the absolute phase [42]. The fact that the count rates in the plateau region are 100–1,000 times lower than for direct electrons is not a real problem. An ATI phasemeter can be built in such a way that even a 30- μ J pulse will produce hundreds of plateau electrons.

In contrast to direct electrons, however, it does not appear to be a good idea to use only electrons beyond the $10-U_P$ cutoff because of the low abundance. Nevertheless, the ATI plateau cutoff energy is the most obvious feature to investigate. Figure 2.13 displays its dependence on absolute phase for 2-cycle pulses. In Fig. 2.14 the dependence of the maximum and minimum cutoff on pulse duration is shown. While these figures certainly have some

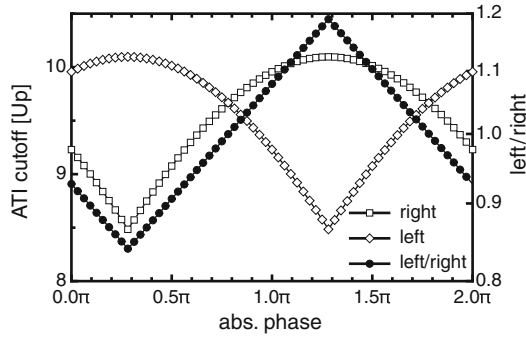


Fig. 2.13. Phase-dependence of the ATI plateau cutoff energy for 2-cycle pulses, i.e., 5.3 fs pulse width (FWHM) at 800 nm. The curves with the open points show the cutoff energy in units of U_P for the spectra measured with the left (*diamonds*) and the right (*squares*) detector. The curve with the solid points displays the ratio of the afore-mentioned curves. Note the logarithmic scale for this curve

⁶ It should be mentioned at this point that for few-cycle conditions the ATI plateau is well-pronounced for Xenon but not so for Argon. Krypton displays the typical plateau only at low intensities [39]. For Helium and Neon experimental data does not seem to be available.

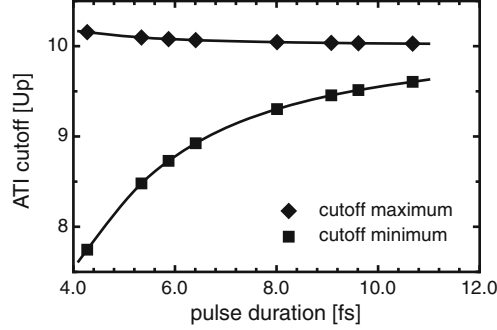


Fig. 2.14. The maximum and minimum cutoff energy as a function of pulse duration. The maximum for electrons emitted to the left is obtained at $\varphi = 0.3\pi$ and the minimum at $\varphi = 1.3\pi$ as shown in Fig. 2.13 for the example of 2-cycle pulses

significance they do not convey the complexity of the entire picture. In fact, each of the strongest cycles creates its own plateau with its own cutoff. The heights of the plateaus depend on the field strength at the time when the respective electron trajectories started. Figure 2.15 gives an impression of the behavior of these cutoffs. Quantum calculations do not exhibit sharp cutoffs (see Fig. 2.16) and it may be difficult to recognize them in cases where the intensity or the ionization probability is low.

For a reasonably complete analysis, interference effects also need to be considered. Interference of trajectories launched by subsequent cycles lead to small-scale fringes with a spacing being given by approximately the photon energy. They are reminiscent and in fact they are closely related to the well-known ATI peak structure and will be discussed in the next paragraph. Large-scale interferences, i.e., interference maxima and minima with an energy separation much bigger than the photon energy, arise from the interference of short and long trajectories: All electron energies below the plateau cutoff can be realized by at least two trajectories of different travel time. The trajectory that is launched later will re-collide earlier and vice versa. These facts are of course well-known from longer pulses. For few-cycle pulses all of the effects cited depend on the absolute phase and many also on pulse duration which makes it difficult to present a concise overview.

Naturally, this has consequences if the phase-dependent ATI plateau is considered for being used to measure the absolute phase. Here one has to distinguish two cases: When the pulse is just to be characterized it is possible to scan the absolute phase from 0 to 2π . In this case the comparison to even classical or semiclassical calculations results in a reliable calibration [42] that is confirmed by all tests that can be performed using other phase-dependent features of ATI spectra. If an ATI phasemeter is to be used in a servo loop, a much faster approach is necessary and the phase cannot be scanned. The safest approach would be to measure the ATI spectra and compare to corresponding

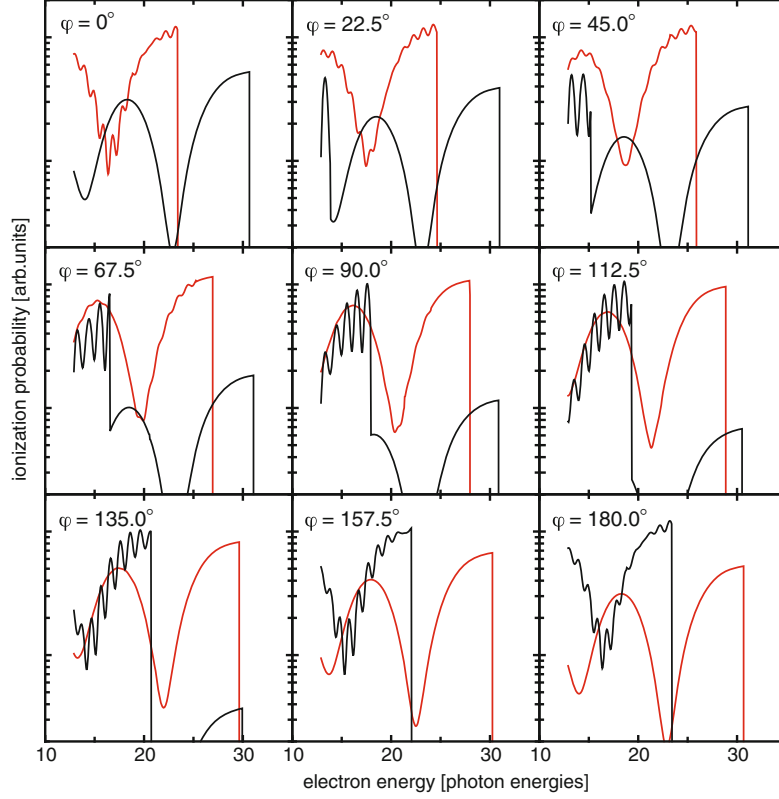


Fig. 2.15. ATI spectra (rescattered electrons only) for various absolute phases calculated with the classical model for a 2-cycle pulse. Interference effects are reproduced by calculating the classical action for the electrons and adding electron trajectories with the same final momentum coherently. One recognizes two types of interferences: Fringes with close to one photon energy separation which arise from wave packets emitted in subsequent optical cycles. In case only one optical cycle leads to significant amplitude for a given electron momentum, the spectrum is smooth. The other type of interference with a fringe spacing of almost 10 photon energies results from interference of long and short electron trajectories. *Black gray* curves correspond to spectra recorded in positive (negative) direction. The intensity is $0.8 \times 10^{14} \text{ W cm}^{-2}$ corresponding to $10 U_P \approx 31 \hbar \omega$. A logarithmic scale is used. [26]

solutions of the TDSE. This, however, is not practical because it seems that Xenon is the preferred atom presently (cf. footnote 6) for which accurate calculations are not available. In addition, focal averaging would need to be included.⁷

⁷ The 1D calculations on which some of the present analysis is based are certainly not suitable for calibrating a phasemeter that takes advantage of ATI plateau electrons. The major reason is that the strength of the plateau for a 1D model atom

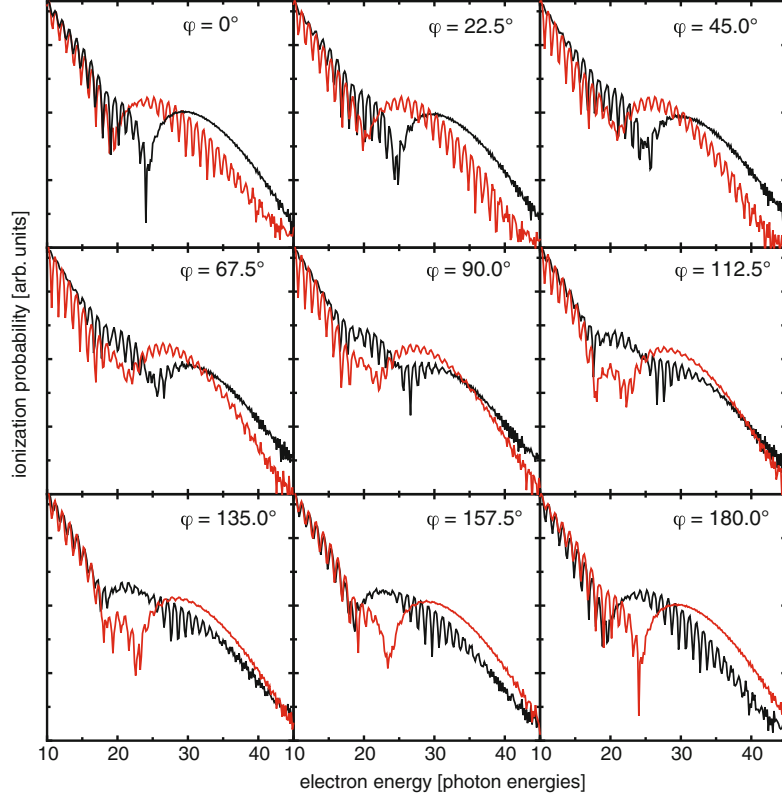


Fig. 2.16. ATI spectra (rescattered electrons only) for various absolute phases calculated with the classical model for a 2-cycle pulse. Interference effects are reproduced by calculating the classical action for the electrons and adding electron trajectories with the same final momentum coherently. One recognizes two types of interferences: Fringes with close to one photon energy separation which arise from wave packets emitted in subsequent optical cycles. In case only one optical cycle leads to significant amplitude for a given electron momentum, the spectrum is smooth. The other type of interference with a fringe spacing of almost 10 photon energies results from interference of long and short electron trajectories. *Black gray curves* correspond to spectra recorded in positive (negative) direction. The intensity is $0.8 \times 10^{14} \text{ W cm}^{-2}$ corresponding to $10 U_P \approx 31 \hbar\omega$. A logarithmic scale is used

2.5 Phase-Dependent Interferences: The Attosecond Double Slit

ATI spectra generated by many-cycle pulses are characterized by a series of peaks separated by the photon energy. The position of these peaks is given by $(N + s)\hbar\omega + E_{\text{Ion}} - U_P$, where N is the number of photons necessary

is considerably smaller than for Xenon. Therefore, the multiple cutoff energies for different optical cycles play a much more pronounced role.

for ionization at zero intensity, s the order of the peak, E_{Ion} the ionization potential, and U_P the ponderomotive energy. Dynamically induced resonances may cause additional peaks. For few-cycle pulses the picture changes in many respects. Figure 2.17 displays measured electron spectra. In Fig. 2.17a the spectra recorded at the left and the right detectors are shown for \pm cosine-like and \pm sine-like pulses as defined in Fig. 2.1. A problem in depicting such spectra is that they quickly roll off with increasing electron energy. This roll-off was eliminated by dividing the spectra by the average of all spectra over the pulse's phase. Peak position, peak contrast, and even peak separation depend on the absolute phase. It seems to be virtually impossible to account for all of these effects within the framework of the conventional theory of ATI.

A better interpretation is based on an analogy to the double-slit experiment. Such an analogy has also been used to interpret multiphoton excitation experiments with Rydberg atoms exposed to microwaves with a variable number of cycles [43]. Here we take advantage of the fact that photoionization of atoms with an ionization threshold much greater than the photon energy is a highly nonlinear process. For intense fields, the first step can be described by optical field ionization, as already noted. This immediately explains that ionization can take place in one attosecond window (or slit) in time per half-cycle close to its extremum. By using phase-controlled few-cycle laser pulses, it is possible to manipulate the temporal evolution of the field, thus gradually opening or closing the slits. In this way which-way information about the instants of ionization is controlled. Depending on the field, one or two half-cycles (or anything in between) contribute to the electron amplitude for a given direction and electron energy. This corresponds to a varying degree of which-way information and, accordingly, to varying contrast of the interference fringes. The temporal slits leading to electrons of given final momentum are spaced by approximately the optical period. This results in a fringe spacing close to the photon energy.

Indeed, clear interference fringes with varying visibility are observed as expected from the discussion above. The highest visibility is observed for $-$ sine-like pulses in the positive (“right”) direction. For the same pulses, the visibility is very low in the opposite direction. Changing the phase by π interchanges the role of left and right as expected. The most straightforward explanation is to assume that, for $-$ sine-like pulses, there are two slits and no which-way information for the positive direction and just one slit and (almost) complete which-way information in the negative direction. The fact that the interference pattern does not entirely disappear is caused by the pulse duration, which is still slightly too long to create a perfect single slit. A semi-classical analysis of the problem qualitatively reproduces the effect. However, the fringes are observed in the opposite direction as compared to the prediction of the simple model. Numerical simulations on the other hand faithfully reproduce the observed pattern [19, 44]. Using the effect for phase measurement is questionable as long as it is not completely understood. A more promising application seems to be to use this type of time-domain

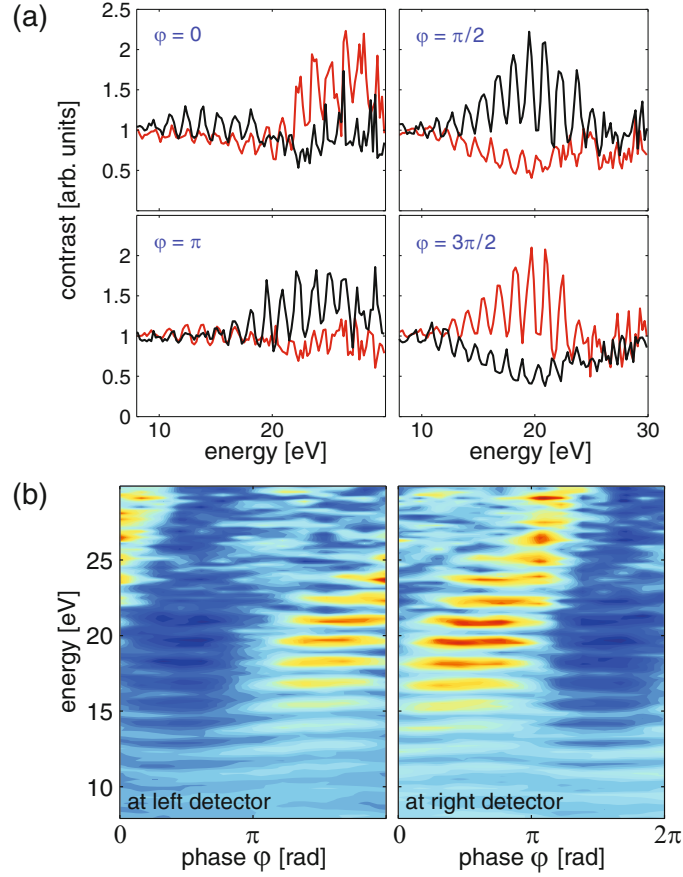


Fig. 2.17. Photoelectron spectra of argon measured with 6-fs laser pulses for intensity $1 \times 10^{14} \text{ W cm}^{-2}$ as a function of the phase. Panel (a) displays the spectra for \pm sine- and \pm cosine-like laser fields. The *gray* curves are spectra recorded with the left detector (negative direction), while the black curves relate to the positive direction. For $\varphi = \pi/2$ the fringes exhibit maximum visibility for electron emission to the right, while in the opposite direction minimum fringe visibility is observed. In addition, the fringe positions are shifted. Panel (b) displays the entire measurement where the fringe visibility is coded in shades of *gray*. The fringe positions vary as the phase φ of the pulse is changed. This causes the wave-like bending of the stripes in these figures. Both panels, in principle, show the same information because a phase shift of π mirrors the pulse field in space and thus reverses the role of positive and negative direction. However, the data shown were recorded simultaneously but independently were the phase φ was varied between 0 and 2π . [44]

interferometry for learning more about the dynamics of the electron wave packet as the ionization process proceeds.

2.6 Conclusions

ATI spectra consist of a low-energy (“direct”) and a high-energy (plateau) part. The latter is due to recolliding electrons, whereas the former is created by electrons that leave the atom directly without a second encounter with the atom. Both parts of the spectrum depend on the absolute phase in a characteristic way. The behavior of plateau electrons is simple in the sense that it can be reproduced by simple classical and semi-classical models. However, there are many different mechanisms that determine the shape of the spectra ranging from the varying amplitude of subsequent optical cycles to interference effects. Surprisingly complicated is the energy-integrated electron yield which is dominated by electrons with close to zero energy. The obvious reason for the difficulties may be that low-energy electrons are more strongly affected by the intra-atomic field which has a strength comparable to the laser field in the vicinity of the atom. The simplest phase-dependence is observed in the cutoff regions for direct and rescattered electrons.

Acknowledgments

I would like to thank the many coworkers and colleagues who helped establishing the, in my opinion, fascinating field of few-cycle quantum optics. In particular, I would like to mention W. Becker, F. Grasbon, F. Krausz, F. Lindner, D. B. Milošević, M. Nisoli, P. Villorosi, and H. Walther. This work was supported by The Welch Foundation (grant A-1562) and the National Science Foundation (grant PHY-0555568).

References

1. M. Ferray, A. L’Huillier, X.F. Li, L.A. Lompré, G. Mainfray, C. Manus, Multiple-harmonic conversion of 1064 nm radiation in rare gases. *J. Phys. B: At. Mol. Opt. Phys.* **21**, L31, 1988
2. G.G. Paulus, W. Nicklich, H. Xu, P. Lambropoulos, H. Walther, Plateau in above threshold ionization spectra. *Phys. Rev. Lett.* **72**, 2851, 1994
3. A. L’Huillier, L.A. Lompre, G. Mainfray, C. Manus, Multiply charged ions induced by multiphoton absorption in rare gases at 0.53 μm . *Phys. Rev. A* **27**, 2503, 1983
4. K.C. Kulander, K.J. Schafer, K.L. Krause, in *Dynamics of Short-Pulse Excitation, Ionization, and Harmonic Conversion*, ed. by B. Piraux, A. l’Huillier, K. Rzazewski. *Super-Intense Laser-Atom Physics*. (Plenum Press, New York, 1993), p. 95

5. P.B. Corkum, Plasma perspective on strong-field multiphoton ionization. *Phys. Rev. Lett.* **71**, 1994, 1993
6. G.G. Paulus, W. Becker, W. Nicklich, H. Walther, Rescattering effects in above-threshold-ionization: a classical model. *J. Phys. B: At. Mol. Opt. Phys.* **27**, L703, 1994
7. P. Salières, A. l’Huillier, P. Antoine, M. Lewenstein, Study of the spatial and temporal coherence of high-order harmonics. *Adv. At. Mol. Opt. Phys.* **141**, 83, 1999
8. W. Becker, F. Grasbon, R. Kopold, D.B. Milošević, G.G. Paulus, H. Walther, Above-threshold ionization: from classical features to quantum effects. *Adv. At. Mol. Opt. Phys.* **48**, 35, 2002
9. R. Dörner, Th. Weber, M. Weckenbrock, A. Staudte, M. Hattass, H. Schmidt-Böcking, R. Moshhammer, J. Ullrich, Multiple ionization in strong laser fields. *Adv. At. Mol. Opt. Phys.* **48**, 1, 2002
10. B. Yang, K.J. Schafer, B. Walker, K.C. Kulander, P. Agostini, L.F. DiMauro, Intensity-dependent scattering rings in high order above-threshold ionization. *Phys. Rev. Lett.* **71**, 3770, 1993
11. I.P. Christov, M.M. Murnane, H.C. Kapteyn, High-harmonic generation of attosecond pulses in the “single-cycle” regime. *Phys. Rev. Lett.* **78**, 1251, 1997
12. M. Hentschel, R. Kienberger, Ch. Spielmann, G.A. Reider, N. Milosevic, T. Brabec, P. Corkum, U. Heinzmann, M. Drescher, F. Krausz, Attosecond metrology. *Nature* **414**, 509, 2001
13. J. Reichert, R. Holzwarth, Th. Udem, T.W. Hänsch, Measuring the frequency of light with mode-locked lasers. *Opt. Commun.* **172**, 59, 1999
14. D.J. Jones, S.A. Diddams, J.K. Ranka, A. Stentz, R.S. Windeler, J.L. Hall, S.T. Cundiff, Carrier-envelope phase control of femtosecond mode-locked lasers and direct optical frequency synthesis. *Science* **288**, 635, 2000
15. T.M. Fortier, P.A. Roos, D.J. Jones, S.T. Cundiff, R.D.R. Bhat, J.E. Sipe, Carrier-envelope phase-controlled quantum interference of injected photocurrents in semiconductors. *Phys. Rev. Lett.* **92**, 147403, 2004
16. O.D. Mücke, T. Tritschler, M. Wegener, U. Morgner, F.X. Kärtner, G. Khitrova, H.M. Gibbs, Carrier-wave Rabi flopping: role of the carrier-envelope phase. *Opt. Lett.* **29**, 2160, 2004
17. A. Apolonski, P. Dombi, G.G. Paulus, M. Kakehata, R. Holzwarth, Th. Udem, Ch. Lemell, K. Torizuka, J. Burgdörfer, T.W. Hänsch, F. Krausz, Observation of light-phase-sensitive photoemission from a metal. *Phys. Rev. Lett.* **92**, 073902, 2004
18. M. Kieß, T. Löffler, M.D. Thomson, R. Dörner, H. Gimpel, K. Zrost, T. Ergler, R. Moshhammer, U. Morgner, J. Ullrich, H.G. Roskos, Determination of the carrier-envelope phase of few-cycle laser pulses with terahertz-emission spectroscopy. *Nature Physics* **2**, 327–331, 2006
19. D.B. Milošević, G.G. Paulus, D. Bauer, W. Becker, Above-threshold ionization by few-cycle pulses. *J. Phys. B: At. Mol. Opt. Phys.* **39**(14), R203–R262, 2006
20. G.G. Paulus, F. Grasbon, H. Walther, P. Villoresi, M. Nisoli, S. Stagira, E. Priori, S. De Silvestri, Absolute-phase phenomena in photoionization with few-cycle laser pulses. *Nature* **414**, 182, 2001
21. D.B. Milošević, G.G. Paulus, W. Becker, Phase-dependent effects of a few-cycle laser pulse. *Phys. Rev. Lett.* **89**, 153001, 2002
22. W. Becker, R.R. Schlicher, M.O. Scully, Final-state effects in above-threshold ionisation. *J. Phys. B: At. Mol. Opt. Phys.* **19**, L785, 1986

23. P. Dietrich, F. Krausz, P.B. Corkum, Determining the absolute carrier phase of a few-cycle laser pulse. *Opt. Lett.* **25**, 16, 2000
24. A.M. Perelomov, V.S. Popov, M.V. Terent'ev. *Sov. Phys. JETP* **24**, 207–217, 1967
25. C.Z. Bisgaard, L.B. Madsen, Tunneling ionization of atoms. *Am. J. Phys.* **72**(2), 249–254, 2003
26. G.G. Paulus, F. Lindner, D.B. Milošević, W. Becker, Phase-controlled single-cycle strong-field photoionization. *Phys. Scr.* **T110**, 120–125, 2004.
27. S. Chelkowski, A.D. Bandrauk, A. Apolonski, Phase-dependent asymmetries in strong-field photoionization by few-cycle laser pulses. *Phys. Rev. A* **70**, 013815, 2004
28. S. Chelkowski, A.D. Bandrauk, Sensitivity of spatial photoelectron distributions to the absolute phase of an ultrashort intense laser pulse. *Phys. Rev. A* **65**, 061802(R), 2002
29. J. Tate, Ph. Colosimo, L.F. DiMauro, G.G. Paulus, Phase-dependence of strong-field photoionization with few-cycle laser pulses, 2008 (unpublished)
30. D. Bauer. Private communication, 2006
31. P. Agostini, F. Fabre, G. Mainfray, G. Petite, N.K. Rahman, Free-free transitions following six-photon ionization of xenon atoms. *Phys. Rev. Lett.* **42**, 1127, 1979
32. S.T. Cundiff, Phase stabilization of ultrashort optical pulses. *J. Phys. D: Appl. Phys.* **35**, R43, 2002
33. A. Baltuška, Th. Udem, M. Uiberacker, M. Hentschel, E. Goulielmakis, Ch. Gohle, R. Holzwarth, V.S. Yakovlev, A. Scrinzi, T.W. Hänsch, F. Krausz, Attosecond control of electronic processes by intense light fields. *Nature* **421**, 611, 2003
34. A. Baltuška, G.G. Paulus, F. Lindner, R. Kienberger, F. Krausz. in *Generation and Measurement of Intense Phase-Controlled Few-Cycle Laser Pulses*, ed. by J. Ye, S.T. Cundiff. *Femtosecond Optical Frequency Comb Technology*. (Springer, New York, 2005), pp. 263–313
35. G.G. Paulus, F. Lindner, H. Walther, A. Baltuška, F. Krausz, Measurement of the phase of few-cycle laser pulses. *J. Mod. Opt.* **52**, 221, 2005
36. G.G. Paulus, W. Becker, H. Walther, Classical rescattering effects in two-color above-threshold ionization. *Phys. Rev. A* **52**, 4043, 1995
37. H.B. van Linden van den Heuvell, H.G. Muller, *Multiphoton Processes, Cambridge Studies in Modern Optics*. (Cambridge University Press, Cambridge, 1988), p. 25
38. T.F. Gallagher, Above-threshold ionization in low-frequency limit. *Phys. Rev. Lett.* **61**, 2304, 1988
39. F. Grasbon, G.G. Paulus, H. Walther, P. Villaresi, G. Sansone, S. Stagira, M. Nisoli, S.De Silvestri, Above-threshold ionization at the few-cycle limit. *Phys. Rev. Lett.* **91**, 173003, 2003
40. F. Lindner, G.G. Paulus, H. Walther, A. Baltuška, E. Goulielmakis, M. Lezius, F. Krausz, Gouy phase shift for few-cycle laser pulses. *Phys. Rev. Lett.* **92**, 113001, 2004
41. D.B. Milošević, G.G. Paulus, W. Becker, High-order above-threshold ionization with few-cycle pulse: a meter of the absolute phase. *Opt. Express* **11**, 1418, 2003
42. G.G. Paulus, F. Lindner, H. Walther, A. Baltuška, E. Goulielmakis, M. Lezius, F. Krausz, Measurement of the phase of few-cycle laser pulses. *Phys. Rev. Lett.* **91**, 253004, 2003

- 43. R.B. Watkins, W.M. Griffith, M.A. Gatzke, T.F. Gallagher, Multiphoton resonance with one to many cycles. *Phys. Rev. Lett.* **77**, 2424, 1996
- 44. F. Lindner, M.G. Schätzel, H. Walther, A. Baltuška, E. Goulielmakis, F. Krausz, D.B. Milošević, D. Bauer, W. Becker, G.G. Paulus, Attosecond double-slit experiment. *Phys. Rev. Lett.* **95**, 040401, 2005

Progress in Ultrafast Intense Laser Science
Volume IV

Becker, A.; Li, R.; Chin, S.L. (Eds.)

2009, XII, 266 p., Hardcover

ISBN: 978-3-540-69142-6